Cell Reports
Article

Secreted Stress-Induced Phosphoprotein 1 Activates the ALK2-SMAD Signaling Pathways and Promotes Cell Proliferation of Ovarian Cancer Cells

Chia-Lung Tsai,[1] Chi-Neu Tsai,[2] Chiao-Yun Lin,[1] Hsi-Wen Chen,[1,3] Yun-Shien Lee,[4,5] Angel Chao,[1,*] Tzu-Hao Wang,[1,3,4,*] Hsin-Shih Wang,[1,2] and Chyong-Huey Lai[1]

[1]Department of Obstetrics and Gynecology, Chang Gung Memorial Hospital and Chang Gung University College of Medicine, Kwai-Shan Taoyuan Taiwan 333, Republic of China
[2]Graduate Institute of Clinical Medical Sciences
[3]Graduate Institute of Biomedical Sciences
Chang Gung University, Kwai-Shan Taoyuan, Taiwan 333, Republic of China
[4]Genomic Medicine Research Core Laboratory, Chang Gung Memorial Hospital, Taoyuan, Taiwan 333, Republic of China
[5]Department of Biotechnology, Ming-Chuan University, Taoyuan, Taiwan 333, Republic of China
*Correspondence: angel945@cgmh.org.tw (A.C.), knoxtn@cgmh.org.tw (T.-H.W.)
http://dx.doi.org/10.1016/j.celrep.2012.07.002

SUMMARY

Stress-induced phosphoprotein 1 (STIP1), a cochaperone that organizes other chaperones, heat shock proteins (HSPs), was recently shown to be secreted by human ovarian cancer cells. In neuronal tissues, binding to prion protein was required for STIP1 to activate the ERK (extracellular-regulated MAP kinase) signaling pathways. However, we report that STIP1 binding to a bone morphogenetic protein (BMP) receptor, ALK2 (activin A receptor, type II-like kinase 2), was necessary and sufficient to stimulate proliferation of ovarian cancer cells. The binding of STIP1 to ALK2 activated the SMAD signaling pathway, leading to transcriptional activation of ID3 (inhibitor of DNA binding 3), promoting cell proliferation. In conclusion, ovarian-cancer-tissue-secreted STIP1 stimulates cancer cell proliferation by binding to ALK2 and activating the SMAD-ID3 signaling pathways. Although animal studies are needed to confirm these mechanisms in vivo, our results may pave the way for developing novel therapeutic strategies for ovarian cancer.

INTRODUCTION

Ovarian cancer is the gynecologic tumor with the highest mortality because most patients with ovarian cancer are diagnosed in advanced stages. Several genes, including BRCA1/2 (breast cancer 1/2, early onset), KRAS, BRAF, and TP53, have been associated with tumorigenesis in ovarian cancer, but their molecular mechanisms remain unclear (Bast et al., 2009). Currently, CA125 is the only tumor marker for monitoring the disease progression of ovarian cancer, but it does not cover all ovarian cancers (Karam and Karlan, 2010). Better understanding of the molecular mechanisms of ovarian cancer may help us develop novel therapeutic strategies.

Stress-induced phosphoprotein 1 (STIP1, STI 1, gene ID 10963), also referred as heat shock protein (HSP) 70/90 organizing protein (HOP), is a 62.6 kDa protein that contains nine tetratricopeptide repeat (TPR) motifs and one nuclear localization signal (NLS) (Longshaw et al., 2004). The TPR domains of STIP1 are involved in holding HSP70 and HSP90 together in the HSP90 chaperone machinery (Odunuga et al., 2004). This formation of protein complexes participates in several cellular processes including transcription, protein folding, protein translocation, viral replication, signal transduction, and cell division (Arbeitman and Hogness, 2000; Bharadwaj et al., 1999; Hu et al., 2002; Johnson et al., 1998; Martins et al., 1997; Zanata et al., 2002). The NLS sequence allows STIP1 transport from cytoplasm to the nucleus under the control of cell-cycle kinases (Longshaw et al., 2004).

STIP1 lacks a transmembrane domain or signal peptide; thus, it was previously considered to be a cytoplasmic protein (Lässle et al., 1997). However, recent studies indicate that it can be translocated to the cell surface or secreted out of the cell (Eustace and Jay, 2004; Wang et al., 2010). Extracellular STIP1 binds to prion proteins on cell surfaces and induces neuroprotective signals that rescue the cell from apoptosis (Roffé et al., 2010; Zanata et al., 2002). In glioblastoma cells, extracellular STIP1 was shown to trigger endogenous mitogen-activated protein kinase 1/2 (ERK1/ERK2), protein kinase A (PKA), and phosphatidylinositol 3-kinase (PI3K) signaling pathways, promoting cell proliferation (Caetano et al., 2008; Erlich et al., 2007; Lopes et al., 2005). Once the interaction between STIP1 and prion protein takes place at the cell surface, the protein is endocytosed, and transient ERK1/ERK2 activation occurs (Caetano et al., 2008).

Bone morphogenetic protein (BMP) pathways are involved in various cell functions, including cell proliferation and migration (Kitisin et al., 2007). These pathways are also important for embryonic development and tumorigenesis (Blanco Calvo et al., 2009; Waite and Eng, 2003). Ligands of the BMP family bind to two distinct membrane receptors, known as type I and type II receptors, which contain serine/threonine kinase domains in their intracellular portions. Upon binding of this ligand, these

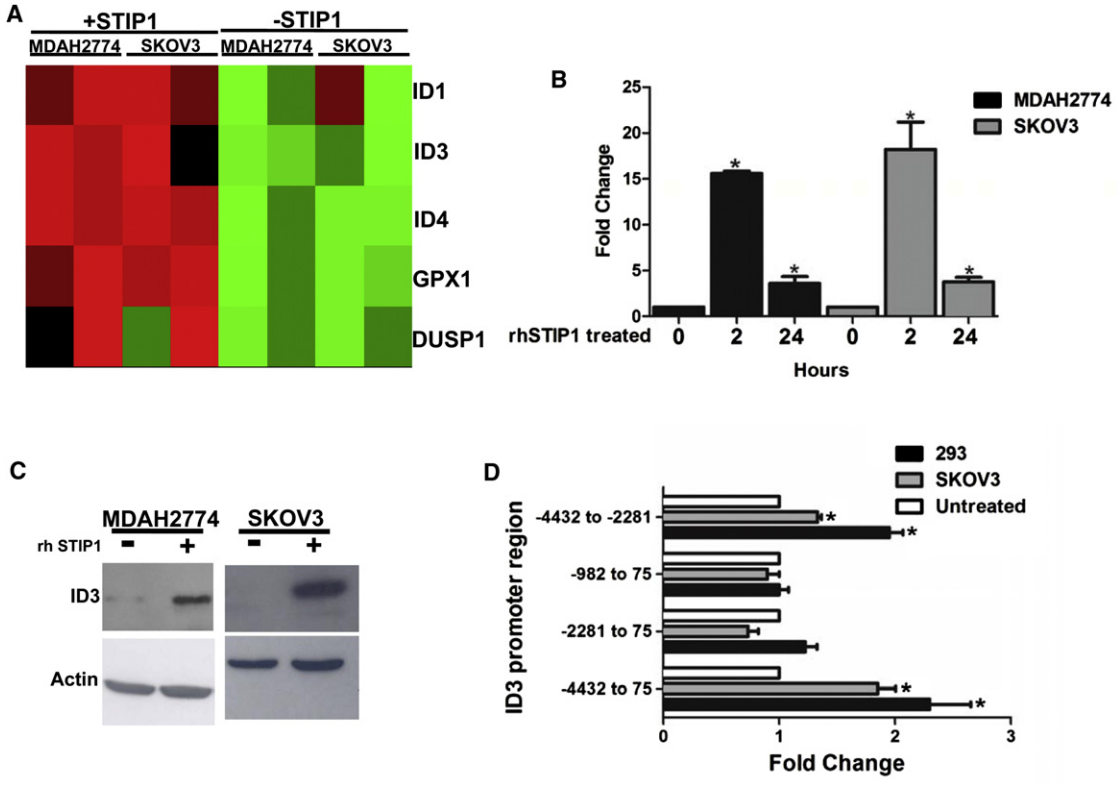

Figure 1. Secreted STIP1 Activated ID3 at the Transcriptional Level

(A) After being cultured in serum-free medium for 24 hr, MDAH2774 and SKOV3 cells were treated with 0.4 μM of rhSTIP1 for 24 hr. The resultant RNAs were analyzed with Affymetrix U133A microarrays. The data shown were obtained from two independent experiments in each cell line.

(B) Activation of ID3 by treatment with STIP1 was confirmed by real-time QPCR at different time points. The data (mean ± SE) shown were obtained from three independent experiments, in which GAPDH was used for normalization purposes. Asterisks denote statistical significance ($p < 0.05$, paired Student's t test).

(C) After MDAH2774 and SKOV3 cells were treated with 0.4 μM of rhSTIP1 for 1 hr, increased ID3 protein levels were detected by western blot analyses. The actin level was used to normalize the input protein.

(D) ID3 promoter luciferase assays were performed in embryonic kidney 293 and SKOV3 cells. Results shown are the mean ± SE of three independent experiments. Asterisks denote statistical significance ($p < 0.05$, paired Student's t test).

See also Table S1 and Figure S1.

two receptors form a hetero-complex where the type II receptor phosphorylates the type I receptor and activates receptor-regulated SMADs (R-SMADs), SMAD1/SMAD5 (Hardwick et al., 2008). Once phosphorylated, SMAD1/SMAD5 form a complex with a common SMAD (co-SMAD), SMAD4 (Heldin et al., 1997). Then, the R-SMADs and co-SMAD complexes are translocated into the nucleus to regulate the transcription of target genes, including IDs (inhibitor of DNA binding) (Miyazono and Miyazawa, 2002). ID proteins compete with the retinoblastoma protein (Rb) to interact with E2F. When E2F is released from Rb, the cell cycle enters the S phase from the G0/G1 phase (Lasorella et al., 2000).

Ovarian cancers produce higher levels of STIP1 than benign tumors do. Because STIP1 is secreted into the blood, the serum STIP1 concentrations in patients with ovarian cancer were significantly higher than those in age-matched controls (Wang et al., 2010). Supporting these findings, Kim and associates found that serum STIP1 autoantibodies were also increased in patients with ovarian cancer (Kim et al., 2010). Treatment of cells with recombinant human STIP1 (rhSTIP1) stimulates ERK1/ERK2 phosphorylation, activates DNA synthesis (Arruda-Carvalho et al., 2007; Erlich et al., 2007), and enhances cell proliferation (Wang et al., 2010). These results suggest that STIP1 in cancer cells acts as a cytokine, with the ability to stimulate cell proliferation.

In this study our microarray results revealed that ID proteins were upregulated by treatment of ovarian cancer cells with rhSTIP1. Interestingly, ERK1/ERK2 was not involved in these STIP1-activated ID pathways. In an attempt to dissect how STIP1 promotes the proliferation of ovarian cancer cells through an ERK-independent pathway, we found that STIP1 binds to a BMP receptor, activin A receptor, type II-like kinase 2 (ALK2) (the updated gene symbol as ACVR1, gene ID 90), and activates ID proteins via the SMAD signaling pathway.

RESULTS

STIP1 Activated Expression of ID1, ID3, and ID4 in Ovarian Cancer Cells

From microarray analysis of gene expression, we found that five genes were upregulated by treatment with rhSTIP1 for 24 hr in MDAH2774 and SKOV3 (Figures 1A and S1; Table S1). ID3 gene

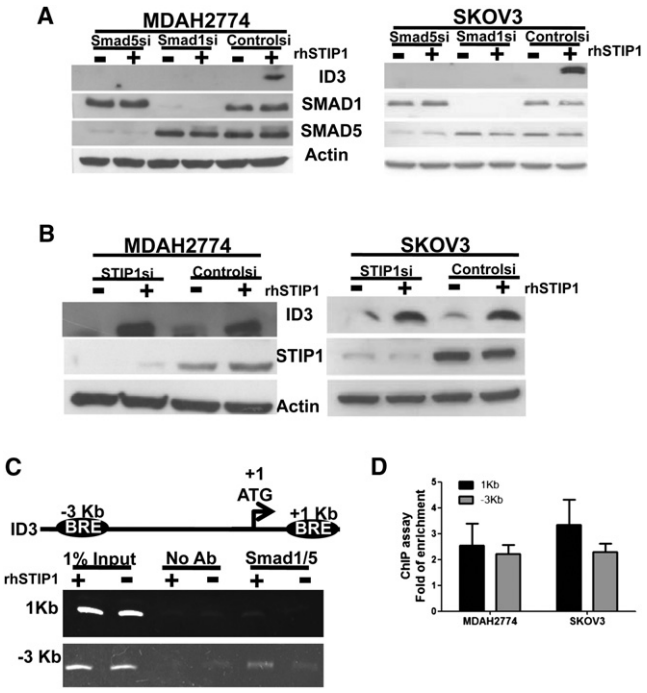

Figure 2. Secreted STIP1 Activated ID3 through SMAD Proteins

(A) Knockdown of endogenous SMAD1 and SMAD5 by siRNA decreased the stimulation of ID3 protein levels by treatment with 0.4 μM of rhSTIP1.

(B) Suppression of endogenous STIP1 by siRNA did not affect ID3 stimulation by rhSTIP1.

(C) STIP1-induced binding of SMADs to two ID3 promoter regions was assayed with ChIP assays with anti-SMAD1/SMAD5 antibody. Two putative SMAD1/SMAD5-responsive elements (BREs) in ID3 promoter region are depicted in the upper panel. The PCR products were separated by 5% nondenature acrylamide gel.

(D) Two reported SMAD binding sites in ID3 promoter are at the 1 kb region (shown in black bar) and the −3 kb region (shown in gray bar). Three independent ChIP experiments were quantified by real-time QPCR, and results shown are mean ± SE.

See also Figure S2.

that promotes cell proliferation was markedly activated by treatment with rhSTIP1 in ovarian cancer cell lines (Figure 1A). STIP1-activated expression of ID3 was further validated by real-time quantitative PCR (QPCR) at different time points (Figure 1B). Also, the amount of ID3 protein was increased by treatment with rhSTIP1 in ovarian cancer cells (Figure 1C). Results of the ID3 promoter reporter assays indicated that STIP1 stimulated the full-length activity from 1.9- to 2.3-fold. The reporter activities were decreased in the truncated promoters: down from 1.3- to 2.0-fold for the −4,432 to −2,281 reporter, 0.7- to 1.2-fold for the −2,281 to +75 reporter, and no activation for the −982 to +75 reporter (Figure 1D). These results suggested that the STIP1 response element is located in the −4,432 to −2,281 region of the ID3 promoter, where several SMAD binding sites are located.

The SMAD Signaling Pathways, but Not ERK Pathways, Were Involved in the Activation of ID Proteins by STIP1

Our previous results indicated that STIP1 activates ERKs (Wang et al., 2010), so we used the ERK-specific inhibitor, PD98059, to test whether the ERK pathway was involved in the activation of ID proteins. Surprisingly, treatment with PD98059 did not significantly inhibit the effective activation of ID3 mRNA by rhSTIP1 treatment (Figure S2A), and the stimulation of pSMAD1/pSMAD5 by rhSTIP1 was not significantly suppressed by PD98059, either (Figure S2B). Because SMAD proteins were shown to be involved in the activation of ID proteins in ovarian cancer (Herrera et al., 2009; Shepherd et al., 2008), we used RNAi to examine the roles of SMAD proteins in the activation of ID3 protein by STIP1. Knocking down SMAD1 and SMAD5 significantly suppressed the activation of ID proteins by rhSTIP1 (Figure 2A). We also checked the role of endogenous STIP1 in ID3 stimulation with small interfering RNA (siRNA) technology. After expression of endogenous STIP1 was suppressed, we still observed the stimulation of ID3 by rhSTIP1 (Figure 2B).

Because there are two BMP-responsive elements (BREs) in the ID3 gene (Shepherd et al., 2008), we used anti-SMAD1/SMAD5 antibodies in chromatin immunoprecipitation (ChIP) assays to test whether STIP1 activated the binding of SMAD proteins to the enhancer region of the ID3 gene. Real-time QPCR results confirmed that treatment of cancer cells with rhSTIP1 increased the binding of SMAD proteins to the 1 and the −3 kb enhancer regions of ID3 gene (Figures 2C and 2D). Taken together, these results indicate that STIP1 activates the expression of ID3 through the SMAD proteins.

STIP1 Induced Phosphorylation of Endogenous SMAD1/SMAD5 in Ovarian Cancer Cells

Treatment of human ovarian cancer MDAH2774 cells with rhSTIP1 induced phosphorylation of SMAD1/SMAD5 in time-dependent (Figure 3A) and dose-dependent (Figure 3B) fashions. The induction of SMAD phosphorylation by rhSTIP1 was also detected in six other human ovarian cancers (Figure 3C). These results indicated that STIP1 activates the canonical SMAD1/SMAD5 pathway in ovarian cancer cells.

Binding to ALK2 Receptors Was Required for STIP1-Induced Phosphorylation of SMAD1/SMAD5

To test whether the prion protein was required for the phosphorylation of SMAD proteins by STIP1, we knocked down the prion protein with siRNA. The knockdown of prion did not suppress the STIP1-induced phosphorylation of SMAD1/SMAD5 (Figure S3). On the other hand, 5 nM of the BMP receptor and serine/threonine kinase inhibitor, LDN193189, effectively blocked the STIP1-induced phosphorylation of SMADs (Figure 4A).

LDN193189 preferentially inhibits ALK2 and ALK3 (IC_{50} = 5 and 30 nM, respectively) but only weakly inhibits ALK4, ALK5, and ALK7 (IC_{50} > 500 nM) (Yu et al., 2008). Knockdown of ALK2 blocked STIP1-activated SMAD1/SMAD5 phosphorylation (Figure 4B), suggesting that the BMP receptor ALK2 is required for STIP1 to activate ovarian cancer cells. Colocalization of rhSTIP1 and ALK2 was also observed by confocal immunofluorescent microscopy (Figure 4C). Because some colocalized signals were found intracellularly after rhSTIP1 treatment for 15 min, we tested whether endocytosis was important for rhSTIP1-induced SMAD1/SMAD5 phosphorylation. As an inhibitor of dynamins, Dynasore blocks the formation of clathrin-coated vesicles (Macia et al., 2006). Clathrin-dependent

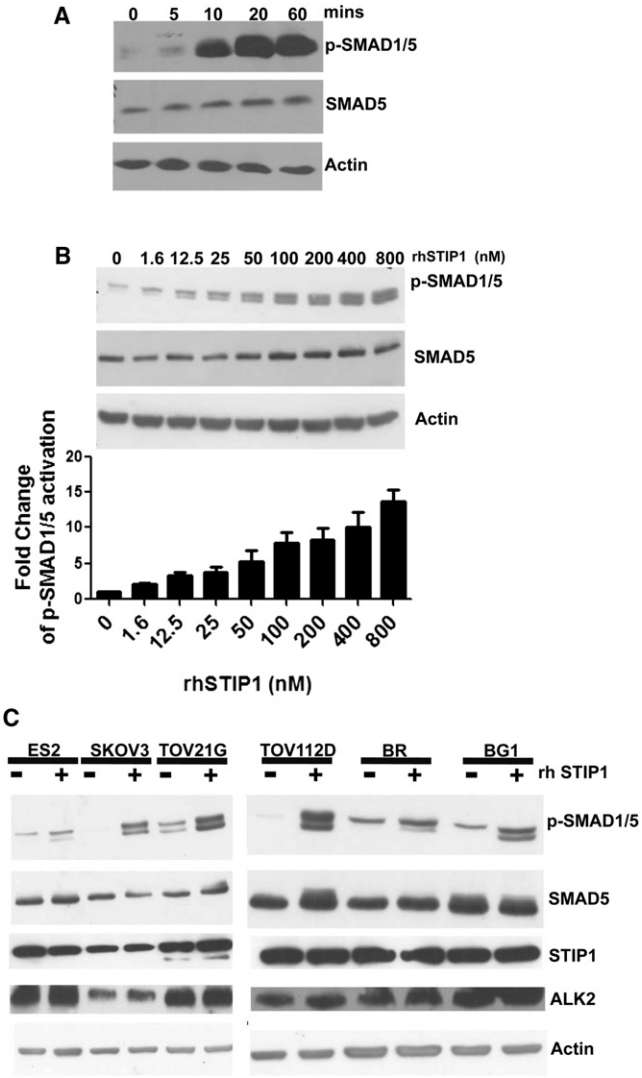

Figure 3. Secreted STIP1 Activated Phosphorylation of Endogenous SMAD1/SMAD5

(A) MDAH2774 cells were serum starved for 24 hr and then treated with 0.4 μM of STIP1 for 0, 5, 10, 20, and 60 min. The phospho-SMAD1/SMAD5 intensities were assayed by western blot analyses. The total amount of SMAD5 and actin was used as the protein loading control.

(B) After serum starvation for 24 hr, MDAH2774 cells were treated with various concentrations of rhSTIP1 for 20 min, and assayed for the activation of phospho-SMAD1/SMAD5 (upper panel). Summary of dose-responsive activation of phospho-SMAD1/SMAD5 by treatment with rhSTIP1 for 20 min (lower panel). Results shown are the mean ± SE from three independent experiments.

(C) Activation of phospho-SMAD1/SMAD5 by treatment with 0.4 μM of rhSTIP1 for 20 min in six other ovarian cancer cell lines.

internalization was also required for BMP-SMAD signal transduction (Hartung et al., 2006; Sieber et al., 2009). The interaction between rhSTIP1 and clathrin was also observed in confocal immunofluorescent microscopy (Figure 4C). The interaction of rhSTIP1 and ALK2 was disrupted (Figure 4C), and the induction of phospho-SMAD1/SMAD5 by rhSTIP1 was repressed by treatment of Dynasore (Figure 4D), suggesting that clathrin-dependent endocytosis was required for the STIP1-activated ALK2-SMAD signaling pathway. Physical interactions between rhSTIP1 and ALK2 were further confirmed by immunoprecipitation (Figure 4E) and pull-down experiments (Figure S3B) followed by western blot analyses (Figures 4E and S3B). To verify that phospho-SMADs were specifically induced by the interaction between STIP1 and ALK2, we used a STIP1-neutralizing antibody and ALK2 fusion protein to block the rhSTIP1 activation of the SMAD pathway. At the molarity ratio between anti-STIP1 antibody and rhSTIP1 at 2:1, rhSTIP1-induced SMAD1/SMAD5 phosphorylation decreased, and such phosphorylation was completely blocked at the ratio of 4:1 (Figure 4F). Similarly, the ALK2-Fc fusion protein at 8-fold molar ratio (ALK2-Fc fusion protein, rhSTIP1 at 8:1) suppressed the rhSTIP1-activated SMAD1/SMAD5 phosphorylation, and the ALK2-Fc fusion protein at a molar ratio of 16:1 completely blocked SMAD1/SMAD5 phosphorylation (Figure 4G). These results collectively indicated that exogenous STIP1 activated the phosphorylation of SMAD1/SMAD5 through its binding to ALK2 receptor, but not through binding to prion protein as previously reported by Zanata et al. (2002).

STIP1 Induced Cell Proliferation through the ALK2-SMAD Pathway

BrdU is an analog of thymidine that can replace thymidine during DNA replication, and Ki67 is a nuclear protein that is associated with cell proliferation. We used BrdU incorporation assay and immunocytochemistry for endogenous Ki67 as indicators for cell proliferation (Wang et al., 2010). Treatment with rhSTIP1 increased the BrdU incorporation rate and Ki67 staining of ovarian cancer cells, and these activations were completely blocked by treatment with an ALK2/ALK3 inhibitor LDN193189 (Figures 5A and 5B), a STIP1-neutralizing antibody (Figures 5C and 5D), or an ALK2 siRNA (Figures 5E and 5F). Of note, inhibition of ERK activity by PD98059 strongly inhibited cell proliferation, but even in such inhibition, treatment with rhSTIP1 still significantly stimulated BrdU incorporation (Figure 5A). These results indicated that ERK pathways are very important for cell proliferation, but the ALK2-SMAD might be more specific for the rhSTIP1-stimulated cell proliferation. Furthermore, knockdown of endogenous STIP1 alone did not inhibit cell proliferation and neither did it affect the stimulation of cell proliferation by treatment with exogenous rhSTIP1 (Figures 5E and 5F).

Serum STIP1 concentrations were previously shown to be higher in patients with ovarian cancer than age-matched healthy controls (Wang et al., 2010). To further confirm that ovarian cancer tissues were the source of elevated serum STIP1, we showed that serum levels of STIP1 in patients with ovarian cancer were significantly decreased after surgery ($p < 0.01$) (Figure 6A). Immunohistochemical analyses of human ovarian cancer tissues also demonstrated that increased levels of STIP1 were positively correlated with increased amounts of phospho-SMAD1/SMAD5 proteins and ID3 (Figure 6B). Notably, ALK2 staining was also shown in the nucleus, as previously reported in the Human Protein Atlas (http://www.proteinatlas.org/ENSG00000115170). Functions of such ALK2 are yet to be clarified. Significantly positive correlations were found between

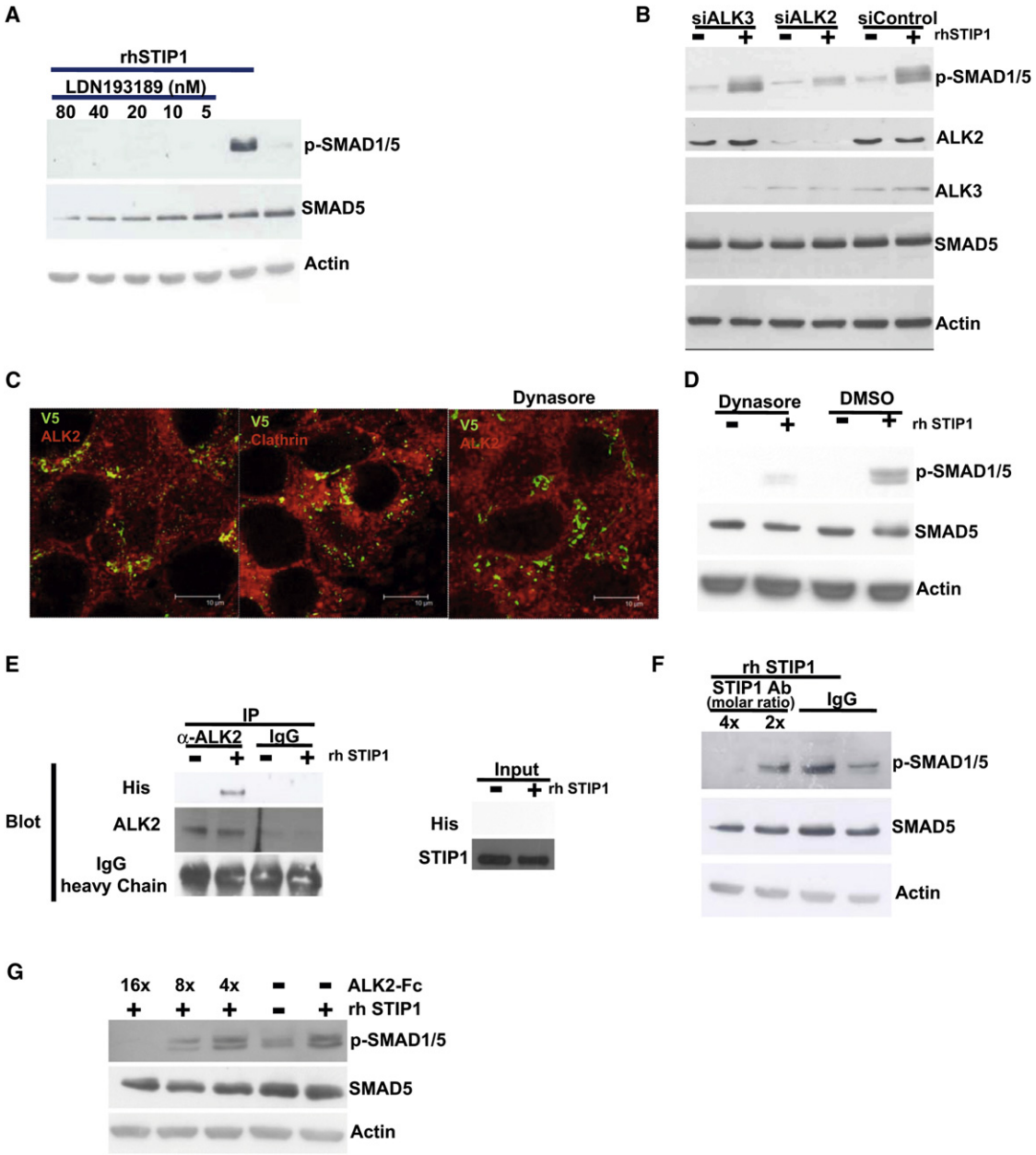

Figure 4. Secreted STIP1 Activated SMAD1/SMAD5 through Binding to a BMP Type I Receptor ALK2

(A) A BMP type I receptor inhibitor, LDN193189, inhibited the STIP1-activated phosphorylation of SMAD1/SMAD5. MDAH2774 cells were pretreated with various concentrations of LDN193189 for 24 hr, before 0.4 μM of rhSTIP1 was added for 20 min.

(B) Knockdown of ALK2 with siRNA inhibited the rhSTIP1-activated phosphorylation of SMAD1/SMAD5.

(C) Intracellular colocalization of exogenous STIP1 (green) and endogenous ALK2 (red, left panel), clathrin (red, middle panel) or endogenous ALK2 in the presence of Dynasore (red, right panel) shown by confocal microscopy. After ovarian cancer cells were treated with rhSTIP1 for 15 min, exogenous STIP1 was detected with an antibody that recognized the V5 tag of rhSTIP1 (green), whereas ALK2 or clathrin was detected by an anti-ALK2 or anti-clathrin antibody (red).

(D) Endocytosis was essential for rhSTIP1-induced SMAD1/SMAD5 phosphorylation. Cells were pretreated with endocytosis inhibitor-Dynasore for 2 hr, then treated with 0.4 μM of rhSTIP1 for 20 min.

(E) After proteins in the rhSTIP1-treated cells were crosslinked, the protein complex around ALK2 from 2,000 μg of protein lysate was immunoprecipitated with specific anti-ALK2 (α-ALK2) antibody, and exogenous rhSTIP1 was identified by western blot analysis with an anti-His tag antibody. A total of 50 μg of identical protein lysates was used as loading control and probed with anti-His and anti-STIP1 antibodies.

(F and G) STIP1-neutralizing antibody and ALK2-Fc inhibited the rhSTIP1-induced SMAD1/SMAD5 phosphorylation. rhSTIP1 was preincubated with antibody or ALK2-Fc for 1 hr at 37°C, then added to cells for 20 min. Western blots were performed with indicated antibodies.

See also Figure S3.

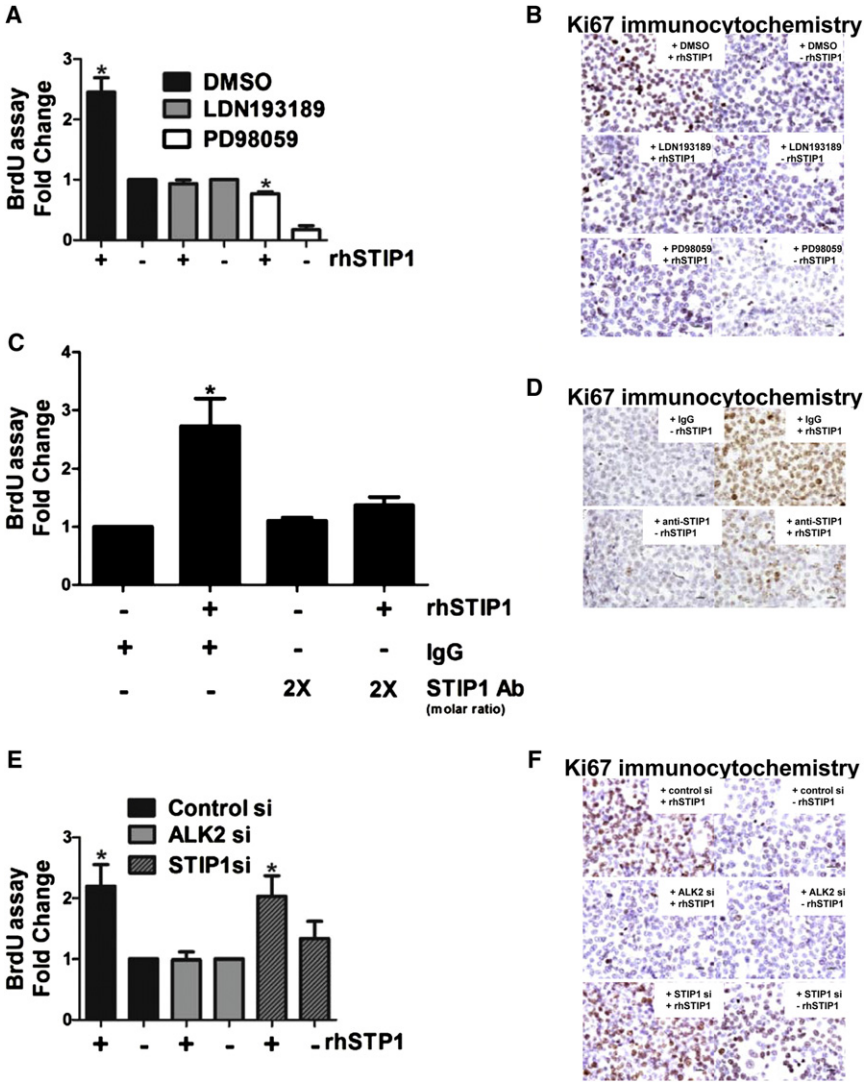

Figure 5. STIP1-ALK2-SMAD Pathway Promoted Cell Proliferation

BrdU incorporation assay and immunointensity of Ki67 protein (brown) were used as an index for cell proliferation. (A), (C), and (E) summarize the results of BrdU incorporation assays, and (B), (D), and (F) show representative pictures of Ki67 immunocytochemistry of MDAH2774 cancer cells treated with ALK inhibitor, LDN 193189, ERK inhibitor PD98059 (A and B), STIP1-neutralizing antibody (C and D), ALK2 siRNA, and STIP1si (E and F), respectively. Results shown are the mean ± SE from three independent experiments. Asterisks denote statistical significance ($p < 0.05$, paired Student's t test). The scale bars represent 20 μm.

STIP1 and phospho-SMAD1/SMAD5 expression ($p < 0.005$; Figure S4A), between ID3 and phospho-SMAD1/SMAD5 ($p < 0.001$), and between STIP1 and ID3 expression ($p < 0.0001$; Figure S4C). Collectively, these results suggest that, after STIP1 is secreted from ovarian tumor tissues, it binds to the ALK2 receptor of itself (autocrine) and/or neighboring cells (paracrine) and triggers SMAD1/SMAD5 to activate ID3 expression in vivo.

DISCUSSION

In this study, we demonstrated that, in an autocrine and/or paracrine fashion, secreted STIP1 from human ovarian cancer cells binds to a BMP receptor, ALK2, phosphorylates cytoplasmic SMAD1/SMAD5, and activates ID3 gene expression, promoting cell proliferation. Marked phosphorylation of SMAD1/SMAD5 was induced by STIP1 at 10 min, and this effect lasted up to 1 hr (Figure 3A). This pattern is similar to that of BMP7 and BMP9, in which these two proteins stimulated phosphorylation of endogenous SMAD1/SMAD5 within 15 min and reached the maximum between 30 and 60 min (Herrera et al., 2009; Macías-Silva et al., 1998). Although STIP1 was reported to bind to prion protein to activate ERK, PAK, PI3K, and mTOR pathways in cells (Caetano et al., 2008; Erlich et al., 2007; Roffé et al., 2010), our results showed that the prion protein was not required for the STIP1-activated SMAD1/SMAD5 pathway (Figure 4A). Our findings of prion-independent cell stimulation by STIP1 are consistent with a previous report by Arruda-Carvalho et al. (2007).

As a receptor serine/threonine kinase, ALK2 interacts with BMP ligands such as BMP6, BMP7, and BMP9, and phosphorylates the downstream SMAD1/SMAD5 (Ebisawa et al., 1999; Herrera et al., 2009; Macías-Silva et al., 1998). We found that STIP1 colocalized and biochemically interacted with ALK2 and that ALK2 was required for the STIP1-induced SMAD signaling pathway (Figure 4). These results strongly suggest that STIP1 is also a ligand for the ALK2-SMAD pathway, although the protein sequence of STIP1 is very different from that of BMPs.

BMPs regulate a variety of cell functions including proliferation, differentiation, apoptosis, and migration through phosphorylation of SMAD1/SMAD5 (Alarmo and Kallioniemi, 2010), which is also crucial for tumorigenesis in many cancers including ovarian cancer. BMP4 induces epithelial to mesenchymal transition (EMT) in primary human ovarian cancer cells (Thériault et al., 2007) and also stimulates cell proliferation via upregulation of proto-oncogene ID3 in ovarian cancer cells (Shepherd et al., 2008). Upregulated BMP2 in ovarian cancer cells stimulates the expression of ID1, SMAD6, and SNAIL (Le Page et al., 2009). In an autocrine fashion, BMP9 promotes the cell proliferation of immortalized human ovarian surface epithelial cells and cancer cell lines through the ALK2/SMAD1/SMAD4 pathway (Herrera et al., 2009). Carcinoma-associated mesenchymal stem cells (CA-MSCs) from ovarian cancer exhibit increased

expression of BMP2, BMP4, and BMP6, which are required for the in vitro and in vivo MSC-promoted tumor growth (McLean et al., 2011). These results indicate that BMP pathways play an important role in tumor cell proliferation of ovarian cancer. However, this study shows that STIP1 secreted from ovarian cancer tissues, similar to BMPs, promotes tumor cell proliferation through the ALK2-SMAD1/SMAD5 pathway (Figures 4 and 5).

Endogenous STIP1 interacts with HSP90 and participates in HSP90-regulated signaling pathways (Taipale et al., 2010). This interaction was shown to inhibit dimerization of HSP90 N terminal and its ATPase activity (Lee et al., 2012; Li et al., 2011), by which STIP1 may cause arrest of the cell cycle as geldanamycin and its derivative 17-allylaminogeldanamycin (17-AAG) do (Niikura et al., 2006). Indeed, our results showed that knockdown of endogenous STIP1 by siRNA slightly increased cell proliferation (Figures 5E and 5F). Nevertheless, the STIP1-knocked down cells still responded to the treatment with rhSTIP1 and further increased cell proliferation (Figures 5E and 5F). Based on these results, we propose that endogenous (intracellular) STIP1 may slightly suppress the progress of the cell cycle by an inhibitory interaction with HSP90, but exogenous (secreted) STIP1 may bind to cell membrane receptors, prion or ALK2, trigger downstream pathways, and promote cell proliferation.

We previously reported that serum levels of STIP1 in patients with ovarian cancer (137.4 ± 112.7 ng/ml, mean ± SD) were significantly higher than those of age-matched healthy controls (23.8 ± 15.1 ng/ml) (Wang et al., 2010). The highest serum STIP1 concentration in peripheral blood of patients with ovarian cancer was about 1,700 ng/ml (Figure 6A). The serum STIP1 concentrations in patients with ovarian cancer significantly decreased after surgery (Figure 6A), supporting that the cancer tissues were the origin of elevated STIP1. Of note, 1.6 nM (about 100 ng/ml) of STIP1 activated greater than 2-fold of SMAD1/SMAD5 phosphorylation (Figure 3B). Therefore, patients with ovarian cancer likely had increased activation of ALK2-SMAD-ID3 pathway from high-serum STIP1 levels. Indeed, the immunohistochemical results in ovarian cancer tissues (Figure 6B) support this notion.

Our discovery that STIP1, in an autocrine or paracrine fashion, promotes ovarian cancer cell proliferation through the ALK2-SMAD1/SMAD5 signaling pathways may be used as proof for principle for various therapeutic strategies. For example, STIP1 in circulation, more importantly those around the cancer tissues, may be neutralized by specific antibodies (Figures 5C and 5D). ALK2 may be inhibited by competitive inhibition with ALK2-Fc fusion proteins (Figure 4G) or by a specific inhibitor (Figures 5A and 5B). Furthermore, the siRNA technology may be applied to all players of the signaling pathway, from STIP1 to ALK2 (Figures 5E and 5F) to SMADs (Figure 2).

In conclusion, ovarian cancer tissues secrete STIP1 into the local environment and eventually into blood circulation. In an autocrine or paracrine fashion, secreted STIP1 stimulates cancer cell proliferation by binding to a BMP receptor, ALK2, and activating the SMAD-ID3 signaling pathways. These results may be useful for developing further therapeutic strategies for ovarian cancer.

EXPERIMENTAL PROCEDURES

Subjects

After informed consent was obtained from each patient, serum was collected from Taiwanese patients with ovarian cancer before surgery and during the postsurgery follow-up. All of the diagnoses of ovarian cancer were confirmed by pathologists at Chang Gung Memorial Hospital (CGMH). This study was approved by the Institutional Review Board of CGMH (IRB #94-975B, #98-1982B, #98-1995A3).

Culture and Treatment of Cell Lines

Human ovarian cancer cell lines (SKOV3, TOV-21G, TOV 112D, OV-90, MDAH2774) and human embryonic kidney epithelial 293 cells were obtained from the American Type Culture Collection (Manassas, VA, USA). The ovarian cancer cell lines BR (Wang et al., 1998) and BG1 (Geisinger et al., 1989) have been previously described. All cells were cultured in DMEM/F12 with 10% fetal bovine serum and appropriate amounts of penicillin and streptomycin. Protocols for rhSTIP1 purification and treatment have been previously reported (Wang et al., 2010). rhSTIP1 was fused with two tags, 6× histidine and V5, and thus, it could be purified or detected with nickel agarose, anti-his, or anti-V5 antibodies. For the use of specific inhibitors, cells were pretreated with 10 μM of PD98059 (ERK inhibitor; Calbiochem, Merck, Germany) for 1 hr, 80 μM of Dynasore (endocytosis inhibitor; Sigma-Aldrich, St. Louis) for 2 hr, or LDN193189 (ALK2 and ALK3 inhibitor; Stemgent, San Diego, CA, USA) for 24 hr before rhSTIP1 was added.

DNA Transfection and Luciferase Reporter Assays

Protocols for DNA transfection and luciferase reporter assays were previously reported (Wang et al., 2010). Briefly, cells were trypsined and resuspended in serum-free RPMI at the concentration of 10^7 cells/ml. A total of 200 μl of cell suspensions was mixed with 5 μg of reporter DNA and 20 ng of renilla plasmid, transferred to 2 mm gap electroporation cuvette, and pulsed at 120V for 70 ms with BTX ECM2001 (BTX, Canada). Cells were reseeded into 6-well plates and cultured in DMEM/F12 with 0.2% fetal bovine serum overnight. During the next day, cells were treated with rhSTIP1 for 24 hr, and luciferase activity was measured with the Dual-Luciferase Reporter Assay System (Promega, Madison, WI, USA) according to the manufacturer's instructions. Four ID3 promoter reporters, the full-length ID3 promoter construct (nt −4,432 to +75) and three truncated constructs (−2,281 to +75, −982 to +75, and −4,432 to −2,281) (Figure 1C), were kind gifts from Dr. Trevor G. Shepherd of Dalhousie University, Canada (Shepherd et al., 2008).

Transfection of siRNA

MDAH2774 (3×10^5 cells in 6-well plates) was transfected with 50 nM of double-stranded RNA in Lipofectamine RNAimax (Invitrogen, Carlsbad, CA, USA) according to manufacturer's protocol. Small interfering prions, si-ALK2 and si-ALK3, were purchased from Dharmacon (Lafayette, CO, USA). si-STIP1 was purchased from Sigma-Aldrich; si-Smad1 and si-Smad5 were from Invitrogen. After 72 hr of transfection, suppression of targeted genes was confirmed by real-time QPCR and western blot analyses.

Western Blot Analysis

Cell lysates were prepared with RIPA buffer (150 mM NaCl, 20 mM Tris-Cl [pH 7.5], 1% Triton X-100, 1% NP-40, 0.1% SDS, 0.5% deoxycholate) containing freshly added proteinase and phosphatase inhibitors (Bionovas, Toronto). Protein concentrations were assayed with the Bradford method. A total of 50 μg of each sample was electrophoresed in 10% SDS-PAGE and transferred to nitrocellulose membranes. All antibodies were from commercial sources: SMAD1, SMAD4, and SMAD5 (Epitomics, Burlingame, CA, USA); phospho-SMAD1/SMAD5 (Millipore, Billerica, MA, USA); prion, ID3 (Abcam, Cambridge); actin (Sigma-Aldrich); and corresponding horseradish peroxidase-conjugated antibodies (Santa Cruz Biotechnology, Santa Cruz, CA, USA). Enhanced chemiluminescence reagents were from Millipore. The signal intensity of autoradiogram was quantified using the UN-SCAN-IT software (Silk Scientific, Orem, UT, USA), and relative intensity of each sample was normalized by the corresponding actin intensity. For antibody neutralization assay, cells were cultured in serum-free medium for 24 hr and then treated

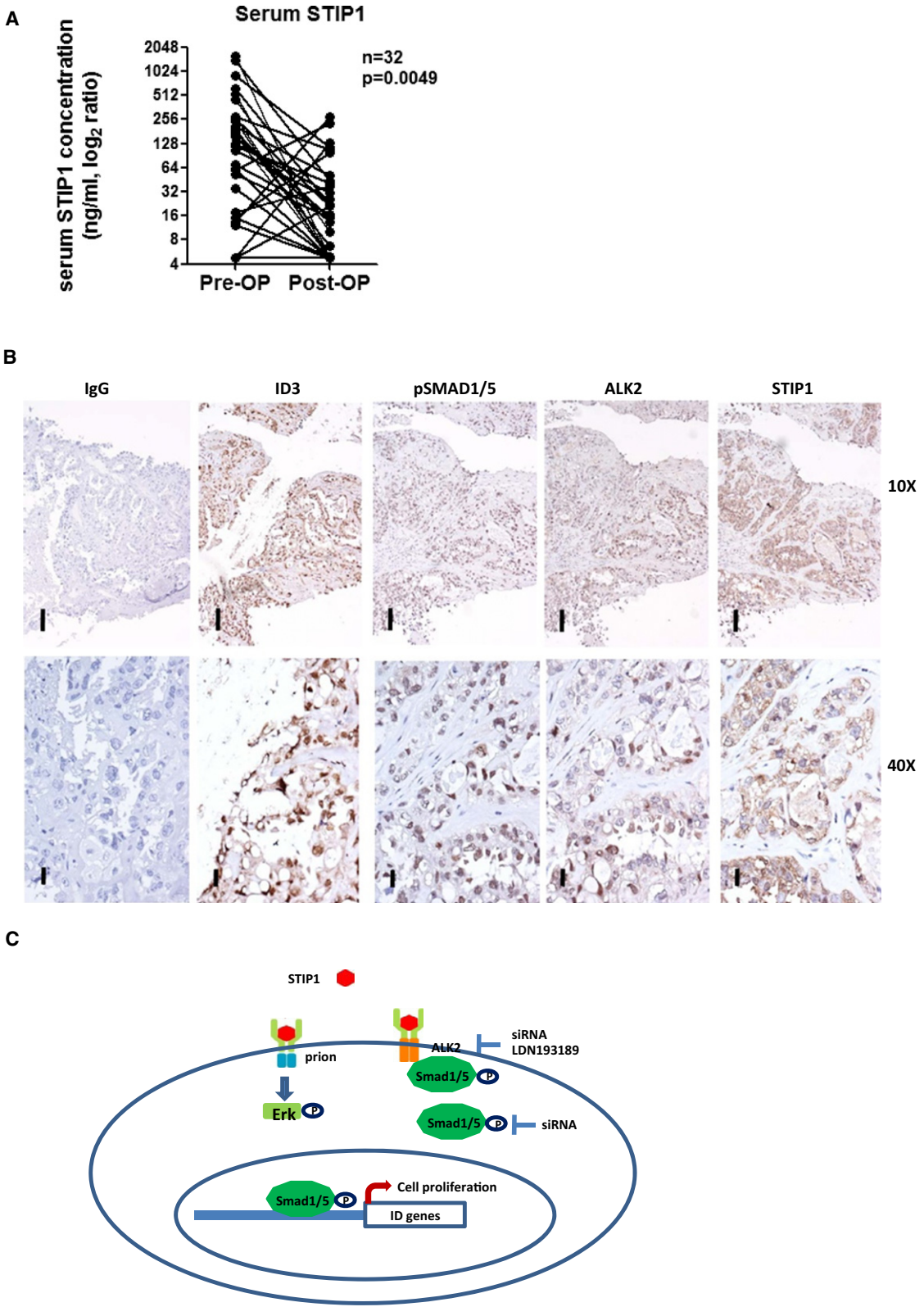

Figure 6. STIP1 Promoted Cell Proliferation through the ALK2-SMAD Signaling Pathway as Shown in Elevated Serum STIP1

(A) The serum levels of STIP1 in patients with ovarian cancer were significantly decreased after surgery (n = 32; p = 0.0049, paired Student's t test).

with rhSTIP1 in the presence or absence of anti-STIP1 monoclonal antibody (Abnova, Taipei, Taiwan) or ALK2-Fc (R&D Systems, Minneapolis) mixtures, which were preincubated at 37°C for 1 hr for 24 hr. Endogenous phospho-SMAD1/SMAD5 were detected by western blot analysis.

RNA Extraction, Microarray Analysis, and Real-Time QPCR

Total RNA was isolated with TRIzol reagent (Invitrogen). Gene expression profiles of the STIP1-treated cells and vehicle-treated control cells were analyzed with a U133A gene chip (Affymetrix, Santa Clara, CA, USA), as previously reported (Tsai et al., 2007). For real-time QPCR, first-strand cDNA was synthesized with an oligo-T primer using SuperScript III First-Strand Synthesis Kit (Invitrogen). Gene expression of ID1, ID3, and GAPDH mRNA was analyzed with the TaqMan Gene Expression Assay (Applied Biosystems, Foster City, CA, USA).

ChIP Assay

Briefly, rhSTIP1-treated or control cells were treated with a final concentration of 1% formaldehyde at RT for 10 min to crosslink proteins to DNA. The reaction was stopped by the addition of glycine (final concentration of 0.125 M). Cells were scraped from the culture dishes into PBS that contained proteinase inhibitors. Cell pellets were resuspended in lysis buffer (5 mM PIPES/KOH [pH 8.0], 85 mM KCL, 0.5% NP-40) and left on ice for 10 min. Nuclei collected by centrifugation were lysed in nuclear lysis buffer (50 mM Tris [pH 8.1], 10 mM EDTA, 1% SDS) and incubated on ice for 10 min. Lysates were sonicated to obtain chromatin with an average length of ~600 bp. After centrifugation, 1 mg of protein supernatant was diluted 5-fold in ChIP dilution buffer (0.01% SDS, 1.1% Triton X-100, 1.2 mM EDTA, 16.7 mM Tris [pH 8.1], 167 mM NaCl). Immunocomplexes were precipitated overnight at 4°C with 5 μg of specific antibodies, followed by five sequential washes with low-salt, high-salt, LiCl, and Tris-EDTA buffer (pH 7.8), respectively (Weinmann et al., 2001). Washed immunoprecipitates were eluted with elution buffer (1% SDS, 0.1 M $NaHCO_3$) at RT, followed by two runs of 15 min vortex and centrifugation. Formaldehyde crosslinks were reversed by incubation in a 65°C water bath for 5 hr. After treatment with Proteinase K followed by phenol/chloroform extraction, DNA fragments were recovered by ethanol precipitation. Immunoprecipitated DNA was amplified by real-time QPCR. The primers used to detect the ID3 enhancer sequence were designed according to a previous report by Shepherd et al. (2008). The following real-time QPCR conditions were used: 95°C for 10 min, 40 cycles of 95°C for 10 s, 60°C for 15 s, and 72°C for 10 s. The SMAD1/SMAD5 antibodies were purchased from Santa Cruz Biotechnology.

Immunohistochemistry

Paraffin-embedded ovarian cancer tissues were sectioned to 4 μm, deparaffinized with xylene, and rehydrated with a series of ethanol solutions. Sections were stained with mouse IgG control, anti-human STIP1 antibody (Abnova), anti-phospho-SMAD1/SMAD5 antibody (Millipore), anti-ALK2 antibody (Santa Cruz Biotechnology), or anti-ID3 antibody (Abcam) in an automated immunohistochemistry (IHC) stainer with Ventana Basic DAB (3,3′-diaminobenzidine) Detection Kit (Tucson, AZ, USA), according to the manufacturer's protocol. Hematoxylin was used for counterstaining. To quantify immunointensity of each IHC slide, histoscores were calculated by multiplying percentage (%) of tumor cells (0%–100%) by immunointensities (0–3), as previously described (Chao et al., 2012).

Ki67 Immunocytochemistry and BrdU Proliferation Assay

Procedures for Ki67 staining and BrdU assay were previously reported (Wang et al., 2010). For BrdU assays, ovarian cancer cells were seeded at a density of 10^4 cells/well in a 96-well plate overnight. After culturing in serum-free medium for 24 hr, cells were treated with 0.4 μM of rhSTIP1 in the presence of BrdU for 24 hr. DNA synthesis activity was assayed using BrdU ELISA kit (Roche Applied Science). For immunocytochemistry studies of Ki-67, MDAH2774 cells were cultured on Lab-Tek II chamber slides (Nalge Nunc, Denmark) overnight. After serum starvation or RNAi transfected for 72 hr, cells were treated with 0.4 μM of STIP1 with/without 5 nM of a BMP inhibitor, LDN193189, or an ERK inhibitor, PD98059, for another 24 hr. The slides were fixed with 99.9% ethanol, rehydrated with PBS, treated with 3% hydrogen peroxide for 20 min, permeabilized with 0.1% Triton X-100 (Sigma-Aldrich) for 15 min, and stained with anti-Ki67 antibody (Thermo Scientific, Rockford, IL, USA).

Immunofluorescent Microscopy

Cells were cultured on cover slides at the concentration of 3×10^5 cells/well in 6-well plates overnight, and underwent serum starvation for another 24 hr. After incubating with 0.4 μM of rhSTIP1 for 15 min at 37°C, cells were fixed with 2% paraformaldehyde at 4°C for 30 min, and incubated in blocking buffer (5% normal goat serum in PBS) to reduce nonspecific binding for 1 hr at RT. For rhSTIP1 and ALK2 staining, cells were incubated with a mouse monoclonal anti-V5 antibody (Invitrogen; 1:100) to detect the V5 and His-fused rhSTIP1 and a rabbit polyclonal anti-ALK2 antibody (Santa Cruz Biotechnology; 1:100), anti-clathrin antibody (Abcam). After incubation with anti-Alexa Fluor 488 (1:100) and anti-mouse Alexa Fluor 546 (1:100; Invitrogen), the slides were mounted with VECTASHIELD mounting medium (Vector Laboratories, Burlingame, CA, USA), and analyzed under the Leica TCS SP2 laser-scanning confocal system (Leica, Germany).

Immunoprecipitation

After serum starvation for 24 hr, MDAH2774 cells were incubated with 0.4 μM of rhSTIP1 for 4 hr at 4°C. Proteins were crosslinked using 1 mM of Disuccinimidyl suberate and Bis(sulfosuccinimidyl)suberate (BS^3) (Thermo Scientific) at 4° for 30 min as previously reported by Greenwald et al. (2003). Cell lysates were prepared with RIPA buffer with proteinase inhibitors, and 2 mg of proteins was incubated with nickel agarose (Invitrogen) at 4°C overnight with agitation. The rhSTIP1 was tagged with V5 and 6× histidine; thus, it adheres to nickel agarose beads. The nickel agarose was washed three times with native wash buffer (50 mM NaH_2PO_4, 500 mM NaCl, 20 mM imidazole [pH 8.0]), and proteins were eluted from the protein complex by native elution buffer (50 mM NaH_2PO_4, 500 mM NaCl, 250 mM imidazole [pH 8.0]). For reversed immunoprecipitation, ALK2 was immunoprecipitated from 2 mg of protein extract by using 2 μg of anti-ALK2 antibody (Santa Cruz Biotechnology), then was performed by ImmunoCruz IP/WB optima system (Santa Cruz Biotechnology). Each sample was electrophoresed with 8% SDS-PAGE. The antibody for ALK2 (Santa Cruz Biotechnology) and the antibody for STIP1 (Abnova) or HIS (Millipore) were used for western blot analysis.

ELISA for STIP1

The development of STIP1 ELISA was reported previously (Wang et al., 2010). Briefly, we used a mouse monoclonal antibody (Abnova) as the capture antibody, which was coated onto 96-well plates (Nunc F8 MaxiSorp, A/S, Roskilde, Denmark). Another biotinylated mouse monoclonal antibody (Abnova) was used as the detection antibody, which could be detected by the Amdex streptavidin-peroxidase conjugate. TMB substrate was used for color formation. The reaction was stopped by the addition of 100 μl/well of 1 N H_2SO_4. Absorbance was determined at 450 nm in a microplate spectrophotometer (Molecular Device SPECTRA Max model 190). The detection sensitivity of our STIP1 ELISA was 2 ng/ml. Intra-assay CVs of the STIP1 ELISA were 4.6% at 59.5 ng/ml (n = 6) and 5.6% at 16.5 ng/ml (n = 6). Interassay CVs were 10.6% at 59.5 ng/ml concentration (n = 7) and 9.4% at 16.5 ng/ml (n = 7).

(B) Colocalization among STIP1, ALK2, phospho-SMAD1/SMAD5, and ID3 in ovarian cancer tissues was shown by IHC. IgG was used as a negative control for the first antibody, and the tissues were counterstained by hematoxylin. Scale bars represent 100 μm in the upper panels of micrographs and 20 μm in the lower panels.

(C) Our working model of activation of the ALK2-SMAD-ID3 pathway by secreted STIP1.

See also Figure S4.

ACCESSION NUMBERS

The data from the microarrays have been deposited to GEO database with accession number GSE27654 (MDAH2774) and GSM892242 (SKOV3).

SUPPLEMENTAL INFORMATION

Supplemental Information includes Extended Experimental Procedures, four figures, and one table and can be found with this article online at http://dx.doi.org/10.1016/j.celrep.2012.07.002.

LICENSING INFORMATION

ACKNOWLEDGMENTS

The authors thank Yi-Jun Lin, Tsung-Ching Wu, Hsiu-Hua Ling, Wei-Chi Chuang, and Chun-An Cheng for technical assistance, the Microscope Core Laboratory, Chang-Gung Memorial Hospital, Linkou for confocal images, Dr. Swei Hsueh (Department of pathology, Chang Gung Memorial Hospital) for pathological expertise on IHC slides, and Dr. Shihtien T. Wang (Department of Kidney Diseases, Northwestern Children's Memorial Hospital, Chicago) for English editing. This study was supported by grants from the National Science Council (NSC99-2321-B-182A-003-MY3 to C.-L.T. and NSC97-2314-B-182A-052-MY3 to T.-H.W.), the Chang Gung Medical Research Foundation (CMRPG391451/2 to A.C., and CMRPG360912 and CMRPG 330313 to T.-H.W.), and the Department of Health (DOH99-TD-I-111-TM013 to T.-H.W. and DOH99-TD-C-111-006 to A.C. and T.-H.W.).

Received: August 19, 2011
Revised: June 22, 2012
Accepted: July 6, 2012
Published online: August 9, 2012

REFERENCES

Alarmo, E.L., and Kallioniemi, A. (2010). Bone morphogenetic proteins in breast cancer: dual role in tumourigenesis? Endocr. Relat. Cancer *17*, R123–R139.

Arbeitman, M.N., and Hogness, D.S. (2000). Molecular chaperones activate the Drosophila ecdysone receptor, an RXR heterodimer. Cell *101*, 67–77.

Arruda-Carvalho, M., Njaine, B., Silveira, M.S., Linden, R., and Chiarini, L.B. (2007). Hop/STI1 modulates retinal proliferation and cell death independent of PrPC. Biochem. Biophys. Res. Commun. *361*, 474–480.

Bast, R.C., Jr., Hennessy, B., and Mills, G.B. (2009). The biology of ovarian cancer: new opportunities for translation. Nat. Rev. Cancer *9*, 415–428.

Bharadwaj, S., Ali, A., and Ovsenek, N. (1999). Multiple components of the HSP90 chaperone complex function in regulation of heat shock factor 1 In vivo. Mol. Cell. Biol. *19*, 8033–8041.

Blanco Calvo, M., Bolós Fernández, V., Medina Villaamil, V., Aparicio Gallego, G., Díaz Prado, S., and Grande Pulido, E. (2009). Biology of BMP signalling and cancer. Clin. Transl. Oncol. *11*, 126–137.

Caetano, F.A., Lopes, M.H., Hajj, G.N., Machado, C.F., Pinto Arantes, C., Magalhães, A.C., Vieira, Mde.P., Américo, T.A., Massensini, A.R., Priola, S.A., et al. (2008). Endocytosis of prion protein is required for ERK1/2 signaling induced by stress-inducible protein 1. J. Neurosci. *28*, 6691–6702.

Chao, A., Lin, C.Y., Lee, Y.S., Tsai, C.L., Wei, P.C., Hsueh, S., Wu, T.I., Tsai, C.N., Wang, C.J., Chao, A.S., et al. (2012). Regulation of ovarian cancer progression by microRNA-187 through targeting Disabled homolog-2. Oncogene *31*, 764–775.

Ebisawa, T., Tada, K., Kitajima, I., Tojo, K., Sampath, T.K., Kawabata, M., Miyazono, K., and Imamura, T. (1999). Characterization of bone morphogenetic protein-6 signaling pathways in osteoblast differentiation. J. Cell Sci. *112*, 3519–3527.

Erlich, R.B., Kahn, S.A., Lima, F.R., Muras, A.G., Martins, R.A., Linden, R., Chiarini, L.B., Martins, V.R., and Moura Neto, V. (2007). STI1 promotes glioma proliferation through MAPK and PI3K pathways. Glia *55*, 1690–1698.

Eustace, B.K., and Jay, D.G. (2004). Extracellular roles for the molecular chaperone, hsp90. Cell Cycle *3*, 1098–1100.

Geisinger, K.R., Kute, T.E., Pettenati, M.J., Welander, C.E., Dennard, Y., Collins, L.A., and Berens, M.E. (1989). Characterization of a human ovarian carcinoma cell line with estrogen and progesterone receptors. Cancer *63*, 280–288.

Greenwald, J., Groppe, J., Gray, P., Wiater, E., Kwiatkowski, W., Vale, W., and Choe, S. (2003). The BMP7/ActRII extracellular domain complex provides new insights into the cooperative nature of receptor assembly. Mol. Cell *11*, 605–617.

Hardwick, J.C., Kodach, L.L., Offerhaus, G.J., and van den Brink, G.R. (2008). Bone morphogenetic protein signalling in colorectal cancer. Nat. Rev. Cancer *8*, 806–812.

Hartung, A., Bitton-Worms, K., Rechtman, M.M., Wenzel, V., Boergermann, J.H., Hassel, S., Henis, Y.I., and Knaus, P. (2006). Different routes of bone morphogenic protein (BMP) receptor endocytosis influence BMP signaling. Mol. Cell. Biol. *26*, 7791–7805.

Heldin, C.H., Miyazono, K., and ten Dijke, P. (1997). TGF-beta signalling from cell membrane to nucleus through SMAD proteins. Nature *390*, 465–471.

Herrera, B., van Dinther, M., Ten Dijke, P., and Inman, G.J. (2009). Autocrine bone morphogenetic protein-9 signals through activin receptor-like kinase-2/Smad1/Smad4 to promote ovarian cancer cell proliferation. Cancer Res. *69*, 9254–9262.

Hu, J., Toft, D., Anselmo, D., and Wang, X. (2002). In vitro reconstitution of functional hepadnavirus reverse transcriptase with cellular chaperone proteins. J. Virol. *76*, 269–279.

Johnson, B.D., Schumacher, R.J., Ross, E.D., and Toft, D.O. (1998). Hop modulates Hsp70/Hsp90 interactions in protein folding. J. Biol. Chem. *273*, 3679–3686.

Karam, A.K., and Karlan, B.Y. (2010). Ovarian cancer: the duplicity of CA125 measurement. Nat. Rev. Clin. Oncol. *7*, 335–339.

Kim, S.H., Cho, H.B., Nam, E.J., Kim, S.W., Kim, Y.T., Park, Y.W., Kim, B.W., and Kim, J.H. (2010). Autoantibodies against stress-induced phosphoprotein-1 as a novel biomarker candidate for ovarian cancer. Genes Chromosomes Cancer *49*, 585–595.

Kitisin, K., Saha, T., Blake, T., Golestaneh, N., Deng, M., Kim, C., Tang, Y., Shetty, K., Mishra, B., and Mishra, L. (2007). Tgf-Beta signaling in development. Sci. STKE *2007*, cm1.

Lasorella, A., Noseda, M., Beyna, M., Yokota, Y., and Iavarone, A. (2000). Id2 is a retinoblastoma protein target and mediates signalling by Myc oncoproteins. Nature *407*, 592–598.

Lässle, M., Blatch, G.L., Kundra, V., Takatori, T., and Zetter, B.R. (1997). Stress-inducible, murine protein mSTI1. Characterization of binding domains for heat shock proteins and in vitro phosphorylation by different kinases. J. Biol. Chem. *272*, 1876–1884.

Lee, C.T., Graf, C., Mayer, F.J., Richter, S.M., and Mayer, M.P. (2012). Dynamics of the regulation of Hsp90 by the co-chaperone Sti1. EMBO J. *31*, 1518–1528.

Le Page, C., Puiffe, M.L., Meunier, L., Zietarska, M., de Ladurantaye, M., Tonin, P.N., Provencher, D., and Mes-Masson, A.M. (2009). BMP-2 signaling in ovarian cancer and its association with poor prognosis. J. Ovarian Res. *2*, 4.

Li, J., Richter, K., and Buchner, J. (2011). Mixed Hsp90-cochaperone complexes are important for the progression of the reaction cycle. Nat. Struct. Mol. Biol. *18*, 61–66.

Longshaw, V.M., Chapple, J.P., Balda, M.S., Cheetham, M.E., and Blatch, G.L. (2004). Nuclear translocation of the Hsp70/Hsp90 organizing protein mSTI1 is regulated by cell cycle kinases. J. Cell Sci. *117*, 701–710.

Lopes, M.H., Hajj, G.N., Muras, A.G., Mancini, G.L., Castro, R.M., Ribeiro, K.C., Brentani, R.R., Linden, R., and Martins, V.R. (2005). Interaction of cellular prion and stress-inducible protein 1 promotes neuritogenesis and neuroprotection by distinct signaling pathways. J. Neurosci. *25*, 11330–11339.

Macia, E., Ehrlich, M., Massol, R., Boucrot, E., Brunner, C., and Kirchhausen, T. (2006). Dynasore, a cell-permeable inhibitor of dynamin. Dev. Cell *10*, 839–850.

Macías-Silva, M., Hoodless, P.A., Tang, S.J., Buchwald, M., and Wrana, J.L. (1998). Specific activation of Smad1 signaling pathways by the BMP7 type I receptor, ALK2. J. Biol. Chem. *273*, 25628–25636.

Martins, V.R., Graner, E., Garcia-Abreu, J., de Souza, S.J., Mercadante, A.F., Veiga, S.S., Zanata, S.M., Neto, V.M., and Brentani, R.R. (1997). Complementary hydropathy identifies a cellular prion protein receptor. Nat. Med. *3*, 1376–1382.

McLean, K., Gong, Y., Choi, Y., Deng, N., Yang, K., Bai, S., Cabrera, L., Keller, E., McCauley, L., Cho, K.R., and Buckanovich, R.J. (2011). Human ovarian carcinoma-associated mesenchymal stem cells regulate cancer stem cells and tumorigenesis via altered BMP production. J. Clin. Invest. *121*, 3206–3219.

Miyazono, K., and Miyazawa, K. (2002). Id: a target of BMP signaling. Sci. STKE *2002*, pe40.

Niikura, Y., Ohta, S., Vandenbeldt, K.J., Abdulle, R., McEwen, B.F., and Kitagawa, K. (2006). 17-AAG, an Hsp90 inhibitor, causes kinetochore defects: a novel mechanism by which 17-AAG inhibits cell proliferation. Oncogene *25*, 4133–4146.

Odunuga, O.O., Longshaw, V.M., and Blatch, G.L. (2004). Hop: more than an Hsp70/Hsp90 adaptor protein. Bioessays *26*, 1058–1068.

Roffé, M., Beraldo, F.H., Bester, R., Nunziante, M., Bach, C., Mancini, G., Gilch, S., Vorberg, I., Castilho, B.A., Martins, V.R., and Hajj, G.N. (2010). Prion protein interaction with stress-inducible protein 1 enhances neuronal protein synthesis via mTOR. Proc. Natl. Acad. Sci. USA *107*, 13147–13152.

Shepherd, T.G., Thériault, B.L., and Nachtigal, M.W. (2008). Autocrine BMP4 signalling regulates ID3 proto-oncogene expression in human ovarian cancer cells. Gene *414*, 95–105.

Sieber, C., Kopf, J., Hiepen, C., and Knaus, P. (2009). Recent advances in BMP receptor signaling. Cytokine Growth Factor Rev. *20*, 343–355.

Taipale, M., Jarosz, D.F., and Lindquist, S. (2010). HSP90 at the hub of protein homeostasis: emerging mechanistic insights. Nat. Rev. Mol. Cell Biol. *11*, 515–528.

Thériault, B.L., Shepherd, T.G., Mujoomdar, M.L., and Nachtigal, M.W. (2007). BMP4 induces EMT and Rho GTPase activation in human ovarian cancer cells. Carcinogenesis *28*, 1153–1162.

Tsai, M.S., Hwang, S.M., Chen, K.D., Lee, Y.S., Hsu, L.W., Chang, Y.J., Wang, C.N., Peng, H.H., Chang, Y.L., Chao, A.S., et al. (2007). Functional network analysis of the transcriptomes of mesenchymal stem cells derived from amniotic fluid, amniotic membrane, cord blood, and bone marrow. Stem Cells *25*, 2511–2523.

Waite, K.A., and Eng, C. (2003). From developmental disorder to heritable cancer: it's all in the BMP/TGF-beta family. Nat. Rev. Genet. *4*, 763–773.

Wang, T.H., Wang, H.S., Ichijo, H., Giannakakou, P., Foster, J.S., Fojo, T., and Wimalasena, J. (1998). Microtubule-interfering agents activate c-Jun N-terminal kinase/stress-activated protein kinase through both Ras and apoptosis signal-regulating kinase pathways. J. Biol. Chem. *273*, 4928–4936.

Wang, T.H., Chao, A., Tsai, C.L., Chang, C.L., Chen, S.H., Lee, Y.S., Chen, J.K., Lin, Y.J., Chang, P.Y., Wang, C.J., et al. (2010). Stress-induced phosphoprotein 1 as a secreted biomarker for human ovarian cancer promotes cancer cell proliferation. Mol. Cell. Proteomics *9*, 1873–1884.

Weinmann, A.S., Bartley, S.M., Zhang, T., Zhang, M.Q., and Farnham, P.J. (2001). Use of chromatin immunoprecipitation to clone novel E2F target promoters. Mol. Cell. Biol. *21*, 6820–6832.

Yu, P.B., Deng, D.Y., Lai, C.S., Hong, C.C., Cuny, G.D., Bouxsein, M.L., Hong, D.W., McManus, P.M., Katagiri, T., Sachidanandan, C., et al. (2008). BMP type I receptor inhibition reduces heterotopic [corrected] ossification. Nat. Med. *14*, 1363–1369.

Zanata, S.M., Lopes, M.H., Mercadante, A.F., Hajj, G.N., Chiarini, L.B., Nomizo, R., Freitas, A.R., Cabral, A.L., Lee, K.S., Juliano, M.A., et al. (2002). Stress-inducible protein 1 is a cell surface ligand for cellular prion that triggers neuroprotection. EMBO J. *21*, 3307–3316.